JOURNAL OF GEOPHYSICAL RESEARCH, VOL. 106, NO. D5, PAGES 4733–4740, MARCH 16, 2001

Development of an inexpensive handheld LED-based Sun photometer for the GLOBE program

David R. Brooks
Department of Mathematics and Computer Science, Drexel University, Philadelphia, Pennsylvania

Forrest M. Mims III
Sun Photometer Atmospheric Network, Seguin, Texas

Abstract. Sun photometers that use light-emitting diode (LED) detectors in place of optical interference filters and photo diodes have significant potential advantages, including low cost, durability, and long-term optical stability. However, their relatively wide spectral response bandwidth poses some challenges in calibration and interpretation. Analysis of LED-based Sun photometers developed for the Global Learning and Observations to Benefit the Environment (GLOBE) program has demonstrated that such instruments can, in fact, be calibrated using the standard Langley plot method and that their performance can be described in terms of effective response wavelengths. Several GLOBE Sun photometers have been calibrated at Mauna Loa Observatory on two separate occasions. The derived extraterrestrial constants are essentially the same in spite of the fact that the calibrations were performed under significantly different atmospheric conditions. These reference instruments have been used to transfer calibrations to other optically and electronically identical Sun photometers, thereby making it possible to establish a large network of inexpensive LED-based Sun photometers. Data collected by students at a GLOBE high school near NASA's Goddard Space Flight Center (GSFC) and compared against aerosol optical thickness measurements from Sun photometers at GSFC demonstrate both that students can reliably make the required measurements and that LED-based Sun photometers give results that compare favorably with conventional filter-based instruments, even though their optical properties are significantly different.

1. Introduction

The concept of handheld Sun photometers was pioneered by *Volz* [1974], and the use of light emitting diodes (LEDs) as inexpensive spectrally selective detectors of light in such devices was first described by *Mims* [1992]. LEDs take the place of interference filters and photo detectors in Sun photometers and require only very simple electronics. LEDs are widely available, inexpensive (typically much less than $1.00 apiece), and rugged and have extremely stable optical properties [*Mims*, 1999]. Interference filters, on the other hand, are expensive, delicate, and prone to optical degradation. Thus, LED-based handheld Sun photometers appear to be ideal instruments for use in a global aerosol monitoring network.

The Global Learning and Observations to Benefit the Environment (GLOBE) program offers the potential for such a network, through thousands of schools in the United States and nearly 100 other countries. (For additional information about GLOBE, see www.globe.gov.) In 1998, GLOBE initiated the Haze/Aerosols Project to develop LED-based Sun photometers to monitor aerosol optical thickness and to train teachers and students in their use [*Mims*, 1999]. The underlying premise of the GLOBE program is that students, motivated by appropriately trained teachers and using detailed written protocols with relatively inexpensive equipment, can provide scientifically valuable measurements of environmental parameters. Most of the equipment GLOBE uses is commercially available, but this is not the case for Sun photometers. Thus a major task for the Haze/Aerosols Project has been to develop a reliable and inexpensive Sun photometer whose performance can be characterized in a way that is acceptable to the atmospheric science community.

Potential applications for a globally distributed network of GLOBE Sun photometers include providing large amounts of information about the background levels and seasonal variability of aerosols over large geographical areas, examining urban/suburban/rural differences in aerosol optical thickness, tracking the movement of dust clouds and volcanic aerosols, and providing ground validation data for satellite-based aerosol retrievals. A two-channel Sun photometer (red and green, for example) can provide information about the size distribution of aerosols. By changing the LEDs, it is also possible to measure aerosol optical thickness in the UV and to measure total column water vapor (by using LEDs that detect light in the near infrared).

Despite their many advantages, LEDs are not necessarily ideal replacements for narrowband optical filters in Sun photometers. Their spectral response bandwidth is much greater than that of interference filters (typically several tens of nanometers versus 10 nm or less), and the wavelengths available are limited to those of commercial devices that are designed for other purposes. Fortunately, a great variety of LEDs is available, with spectral responses from the UV to the near IR. (The relationship between LED emission and detection spectra is not a simple one. In particular, the peak detection wavelength is not, in general, the same as the peak emission wavelength.) Despite these challenges, the potential scientific value of an inexpensive and widely dispersed network of reliable LED-based Sun photometers is so great that it is well worth the effort required to understand their performance.

Paper number 2000JD900545.
0148-0227/01/2000JD900545$09.00

2. Equations

For monochromatic sunlight of wavelength λ transmitted directly through the atmosphere along a narrow path to an observer at the Earth's surface, the intensity seen by an observer at the Earth's surface due to scattering or absorption of light is described by the well-known Beer-Lambert-Bouguer (BLB) law:

$$I_\lambda = (I_{o,\lambda}/r^2)\exp(-\alpha_\lambda m), \quad (1)$$

where $I_{o,\lambda}$ is the intensity of sunlight (in arbitrary units) just above the Earth's atmosphere when the Earth-Sun distance is 1 AU, r is the Earth-Sun distance in units of AU, α_λ is the total atmospheric optical thickness, and m is the relative air mass, normalized to 1 for overhead Sun at the observer's location, and approximately equal to sec(z), where z is the solar zenith angle.

The contributors to total atmospheric optical thickness include Rayleigh (molecular) scattering, absorption by gases, and scattering and absorption by aerosols. Designating the Rayleigh optical thickness by α_R and the non-Rayleigh optical thickness by $\alpha_{a'}$, and assuming that a Sun photometer whose narrowband response is centered around wavelength λ produces a voltage V that is directly proportional to I_λ, equation (1) can be rewritten as

$$V = (V_o/r^2)\exp\left(\frac{-\alpha_{a'} - \alpha_R(p/p_o)}{m}\right), \quad (2)$$

where the wavelength dependence previously indicated by the λ subscript is now assumed without specific notation for each component. In the Rayleigh term, the ratio p/p_o accounts for the fact that Rayleigh scattering coefficients are typically calculated for a standard atmosphere at sea level and, assuming a vertically mixed atmosphere, can be corrected to the observer's elevation. Equation (2) can be solved for $\alpha_{a'}$:

$$\alpha_{a'} = \frac{\ln(V_o/r^2) - \ln(V) - \alpha_R(p/p_o)m}{m}. \quad (3)$$

Separation of the non-Rayleigh term $\alpha_{a'}$ into its components, including aerosols as well as the effects of gaseous absorption, is not a trivial matter.

The contribution due to Rayleigh scattering can, in principle, be derived from the fundamental physics of the atmosphere, although results can differ somewhat because of uncertainties in the analysis of those properties. *Bucholtz* [1995] has produced tabulated values of α_R based on standard atmospheres (U.S. Standard Atmospheres, 1962 and 1966) at sea level and has given analytical representations for those tabulations of form

$$\alpha_R = A\lambda^{-(B + C\lambda + D/\lambda)}, \quad (4)$$

where λ is specified in microns. Table 1 gives values for the four coefficients for the 1962 U.S. Standard Atmosphere; *Bucholtz* [1995] also gives sets of coefficients that depend on latitude and season, but the differences are minor. The number of significant digits shown for the coefficients are mathematical artifacts of the empirical fit to the data and are not all physically significant.

Table 1. Coefficients for Modeling Rayleigh Scattering

Coefficient	Value
A	$260 \le \lambda \le 500$ nm: 6.50362×10^{-3} $\lambda > 500$ nm: 8.64627×10^{-3}
B	$260 \le \lambda \le 500$ nm: 3.55212 $\lambda > 500$ nm: 3.99668
C	$260 \le \lambda \le 500$ nm: 3.55212 $\lambda > 500$ nm: 3.99668
D	$260 \le \lambda \le 500$ nm: 0.11563 $\lambda > 500$ nm: 2.71393×10^{-2}

From *Bucholtz* [1995].

The relative air mass m in (3) is approximately equal to the secant of the solar zenith angle. An equation developed by *Young* [1994] takes into account atmospheric refraction and the effects of a spherical Earth, which are important at large zenith angles:

$$m(z) = \frac{1.002432\cos^2 z + 0.148386\cos z + 0.0096467}{\cos^3 z + 0.149864\cos^2 z + 0.0102963\cos z + 0.000303978}. \quad (5)$$

Solar zenith angle z is calculated from the astronomical position of the Sun [see, e.g., Meeus, 1991], and (5) includes refraction effects for an average atmosphere. The difference between $m(z)$ as given by (5) and sec(z) is not significant for conditions under which Sun photometer measurements are normally made, but it can become significant for conditions under which Sun photometer calibrations are performed. The number of significant digits given for the coefficients in (5) is intended to ensure stable numerical behavior as z approaches 90° and does not imply that the calculation is inherently this accurate. The advantage of an astronomically based model for solar position is that it relieves an observer of the task of measuring solar zenith angle directly. This is an especially difficult task as the Sun approaches the horizon and is likely to produce low-accuracy results when done, as in *Volz*'s [1974] original design, by measuring the length of the sun's shadow produced by a small bracket attached to a handheld instrument.

3. Instrument Calibration and Interpretation of Measurements

LED-based Sun photometers pose challenges for calibration and interpretation because their relatively wide spectral response prohibits indiscriminate application of the BLB law. Understanding the relationship between these instruments and their counterparts that rely on narrowband optical filters is fundamental to their use.

The standard approach to determining a Sun photometer's extraterrestrial constant V_o is the Langley method (as described by *Abbott and Fowle* [1908]), in which the logarithm of the Sun photometer voltage is plotted as a function of relative air mass:

$$\ln(V) = \ln(V_o/r^2) - \alpha_\lambda m. \quad (6)$$

The slope of a linear regression line through the data gives the total atmospheric optical thickness α_λ and the intercept at m=0 gives the logarithm of the extraterrestrial constant for the Earth-Sun distance at the time of measurement.

Figure 1 [from *Mims*, 1999] shows a Langley plot calibration for an LED Sun photometer taken from 29.61°N latitude and 97.93°W longitude at an elevation of 168 m on March 9, 1996. Application of the Langley method requires a stable atmosphere during the several hours required to collect the data. These data represent exceptionally stable atmospheric conditions, and they are not typical of calibration data obtained from low-elevation sites.

The Langley calibration method defined in (6) assumes a Sun photometer that satisfies the requirements for the BLB law (a direct beam of monochromatic light). However, actual instruments detect light over a finite wavelength interval. Historically, Sun photometers have typically used interference filters with full-width, half-maximum bandwidths of 10 nm or less, and it has been assumed that the monochromatic assumption is still valid. Following *Reagan et al.* [1987], the corresponding equation for a Sun photometer that does not meet the conditions for the BLB law (in particular, when the light is not even approximately monochromatic) is

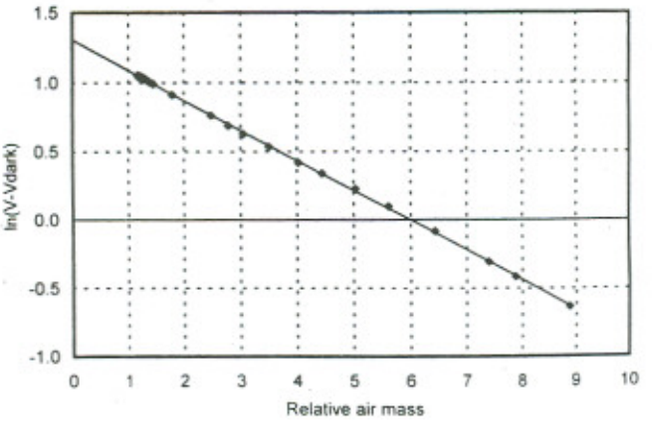

Figure 1. Langley plot calibration for a light-emitting diode (LED) based Sun photometer, from Seguin, Texas, March 9, 1999 (unpublished data from Mims).

$$V = V_o \hat{T}, \tag{7}$$

where $\hat{T}$ is a wideband transmittance function that accounts for the spectral variation of the optical thicknesses associated with molecular scattering, particle scattering, and gaseous absorption. For an instrument whose spectral response extends over a wavelength interval from λ_1 to λ_2,

$$\hat{T} = \frac{\int_{\lambda_1}^{\lambda_2} R_\lambda F_{o,\lambda} \exp(-m_a \alpha_{a,\lambda} - m_R \alpha_{R,\lambda} - m_g \alpha_{g,\lambda}) d\lambda}{\int_{\lambda_1}^{\lambda_2} R_\lambda F_{o,\lambda} d\lambda}, \tag{8}$$

where R_λ is the normalized spectral response of the detector and $F_{o,\lambda}$ is the solar radiation incident at the top of the atmosphere. As noted by *Reagan et al.* [1987], it is not obvious that the transmittance function $\hat{T}$ can be simply represented by an exponential function when $\lambda_2 - \lambda_1$ is large ("100 nm or more") and when gaseous absorption cannot be ignored.

Figure 2 shows the spectral response of several LEDs. An important message from Figure 2 is that it is not sufficient simply to select "green" or "red" (or some other color) LEDs at random for use in LED-based Sun photometers. The figure shows that there are differences in spectral response that are critical for this application. In particular, smaller full-width half-maximum (FWHM) bandwidths are preferred over wider bandwidths. Of the LEDs shown in Figure 2, the Agilent HLMP-D600 (emerald green) and HLMP-3762 (red) are clear choices over other branded and generic LEDs. In fact, generic LEDs should never be used in this application because there is no practical way to exercise quality control over their performance in a widely distributed network. On the other hand, tests on random samples of brand-name LEDs purchased in bulk have shown that spectral response is repeatable from sample to sample within limits that if exceeded, would produce visible differences in Figure 2, for example. Within the GLOBE Haze/Aerosols Project, spectral response data are collected for every batch of LEDs purchased.

It is clear from Figure 2 that LED responses can approach the definition of a "large" bandwidth; the FWHM bandwidth for the HLMP-D600 LED used in the GLOBE Sun photometer is about 75 nm. If it is not possible to represent the transmittance with an exponential function, then total optical thickness can no longer be defined simply as the slope of the graph of $\ln(V)$ as a function of relative air mass and $\ln(V_o/r^2)$ can no longer be linearly extrapolated from photometer data, as is assumed for Langley plot calibrations. Furthermore, transfer calibrations from narrowband filter-based Sun photometers to LED-based photometers, from which an LED-based instrument's extraterrestrial constant can be determined in circumstances when Langley calibrations are not feasible, are greatly complicated.

However, experience with LED Sun photometers shows that Langley plot calibrations are possible when the same atmospheric conditions that apply to other Sun photometers are met. Figure 1 has shown one such calibration. In order to simulate the behavior of LED-based Sun photometers, sums over the 5-nm-wavelength intervals previously used to determine the LED spectral responses R_λ shown in Figure 2 were used as numerical approximations for the integrals in (8). Extraterrestrial solar radiation $F_{o,\lambda}$ was obtained from standard sources and averaged over 5-nm intervals. Ozone optical thickness for a concentration of 300 Dobson units (DU) over the same range of wavelengths was taken from tables of *Iqbal* [1983]. An effective aerosol optical thickness wavelength for a particular detector is defined as a weighted sum over the spectral response:

$$\lambda_{eff} = \frac{\sum_{i=1}^{n} R_{\lambda_i} F_{o,\lambda_i} \lambda_i \Delta\lambda}{\sum_{i=1}^{n} R_{\lambda_i} F_{o,\lambda_i} \Delta\lambda}, \tag{9}$$

where $\Delta\lambda$ is 5 nm over the range of n wavelength intervals for which the LED exhibits a significant response. For the D600 LED shown in Figure 2, λ_{eff} is about 508 nm.

In the simulation, the sums over wavelength are done at several values of relative air mass. If the resulting simulated Langley plot is a straight line, it implies that the wideband transmittance function defined in (8) can be represented as an exponential function of form

$$\hat{T} = \exp(-m\alpha_{\lambda,eff}) = \exp[-m(\alpha_{a,\lambda,eff} + \alpha_{R,\lambda,eff} + \alpha_{g,\lambda,eff})]. \tag{10}$$

Equation (10) assumes not only that voltages measured with a wideband Sun photometer can be linearly extrapolated to zero relative air mass along a line with a slope equal to the negative of the total optical thickness, to obtain the extraterrestrial constant for the instrument, but also that the total optical thickness can be expressed in terms of effective aerosol, molecular, and gaseous absorption components that can be associated with specific wavelengths. Each of the effective wavelengths can be different.

Equation (10) also assumes that the relative air mass is the same for each contributing component, which is equivalent to assuming that the vertical distribution of each component is the same. This is not true, and as noted by *Dutton et al.*, [1994, p. 8299], "The need to know the vertical distribution of the aerosol before optical depth can be more accurately computed is a limit to the remote sensing of aerosol optical depth from the Earth's surface."

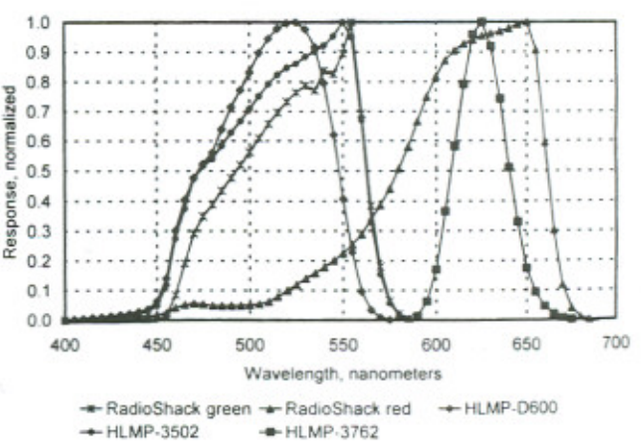

Figure 2. Spectral response of selected LEDs.

Even the assumption of known but different vertical distributions poses a problem for precision Sun photometry. Molecular scattering comes from a vertically well mixed atmosphere that decreases monotonically in concentration from sea level. On the other hand, ozone concentrations peak in the stratosphere, and this gas is sometimes treated as a single layer at an altitude of around 22 km. Other potential scatterers and absorbers may have other vertical distributions. The vertical distribution of aerosols is highly variable. Tropospheric aerosols may be confined to the lower 2-3 km of the atmosphere, but layers of stratospheric aerosols (from volcanic eruptions, for example) lie much higher in the atmosphere. As *Thomason et al.* [1983] have pointed out, if separate values of relative air mass must be retained for each scattering and absorbing component, a Langley calibration as described in (6) is, strictly speaking, no longer possible because there is no longer a linear relationship between intensity (as transformed into signal voltage from a specific instrument) and the logarithm of a representative relative air mass. Nevertheless, these effects are, typically, relatively minor, and simplifying assumptions are routinely made for processing data from operational instruments such as those used in NASA's Aerosol Robotic Network (AERONET) Sun photometer network [*Holben et al.*, 1998]. The simulation described here assumes that the relative air mass is the same for aerosols as for Rayleigh scattering. For ozone, results from Thomason *et al.* (1983) have been used as the basis of an empirical function $c(z)$ to modify ozone relative air mass so that the exponent in (10) can be rewritten in the form $-m(\alpha_{o,\mathrm{eff}} + \alpha_{R,\mathrm{eff}} + c(z)\alpha_{g,\mathrm{eff}})$.

If, in fact, the optical thicknesses due to Rayleigh scattering and gaseous absorption (restricted to ozone for this analysis) can be represented by effective values based on their wavelength dependence over the spectral
response of the detector, then these values are given by

$$\alpha_{R,\mathrm{eff}} = \frac{\int_{\lambda_1}^{\lambda_2} R_\lambda F_{o,\lambda} \alpha_{R,\lambda} d\lambda}{\int_{\lambda_1}^{\lambda_2} R_\lambda F_{o,\lambda} d\lambda}$$

$$\alpha_{g,\mathrm{eff}} = \frac{\int_{\lambda_1}^{\lambda_2} R_\lambda F_{o,\lambda} \alpha_{g,\lambda} d\lambda}{\int_{\lambda_1}^{\lambda_2} R_\lambda F_{o,\lambda} d\lambda}. \quad (11)$$

In practice, the integrals in these definitions are replaced with sums, as in (9).

Note that the purpose of including an ozone component in the analysis is not to imply that an average ozone concentration should be used to separate aerosol optical thickness from total non-Rayleigh optical thickness, but only to examine the effect of a nonaerosol component with a vertical distribution that differs significantly from typical aerosol distributions. In terms of analyzing GLOBE Sun photometer data, satellite-derived ozone concentrations can be used to separate actual ozone contributions to the non-Rayleigh optical thickness.

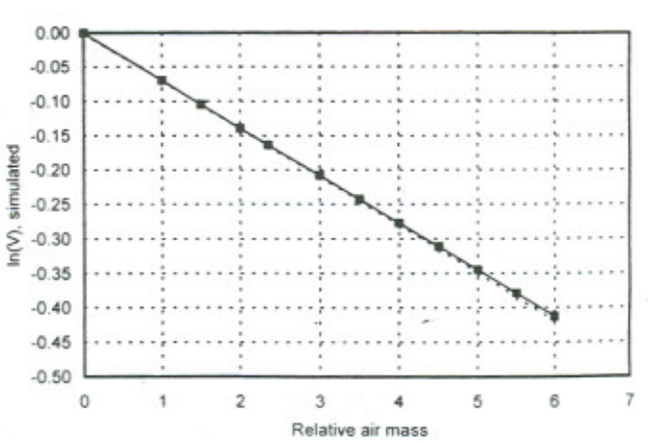

Figure 3. Simulated Langley plot calibrations based on measured spectral response of Agilent HLMP-D600 emerald green LED.

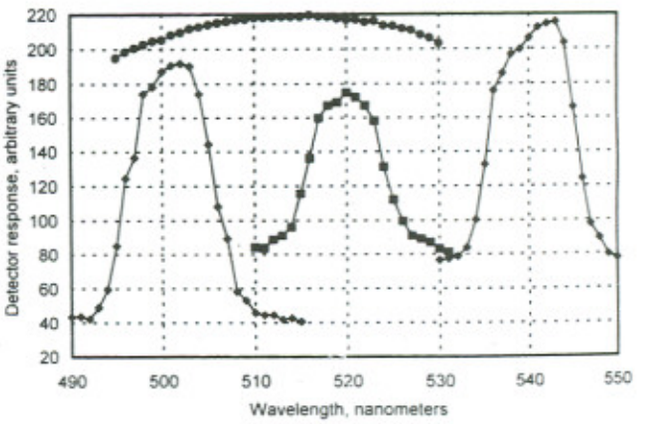

Figure 4. Spectral response for detectors in a modified MicroTops Sun photometer. The detector marked by crosses is the Agilent HLMP-D600 emerald green LED used in the GLOBE Sun photoeter. The others are 10-nm or 80-nm filters.

The effective Rayleigh optical thickness is especially important, as it characterizes the instrument's response to molecular scattering, which is a significant portion of the total atmospheric optical thickness in the range of visible wavelengths. At the wavelength of the green LED used in the GLOBE Sun photometer, $\alpha_{R,\mathrm{eff}}$ corresponds to a wavelength of about 505 nm and the Rayleigh coefficient (from equation (4)) is about 0.138. (In contrast, the non-Rayleigh optical thickness at this wavelength can be less than 0.1 for a clear sky.) Because of the strong wavelength dependence of Rayleigh scattering, decreasing with wavelength, it is not surprising that the weighted Rayleigh wavelength is somewhat less than the wavelength for peak spectral response of the LED. Note that the effective Rayleigh wavelength is slightly different from the effective wavelength for aerosol optical thickness as defined in (9).

4. Langley Plot Calibrations

Equations (8) and (10) provide the information required to generate simulated Langley plots with the goal of determining the extent of any problems associated with assuming effective values of optical depth for aerosols, Rayleigh scattering, and gaseous absorbers.

Figure 3 shows a simulated Langley plot for an assumed aerosol optical thickness of 0.1 at the effective wavelength of 508 nm. The solid line with symbols represents the logarithm of the "actual" voltage the instrument would see, given the assumed properties of the atmosphere. The dashed line, which is distinguishable from the solid line only at relative air masses greater than about 5, is generated from a model using effective values for Rayleigh scattering and ozone absorption. For conditions under which Sun photometer measurements are normally made, the differences are negligible.

5. Side-by-Side Comparisons of LED Detectors and Interference Filters

One way to assess the performance of LED-based Sun photometers is to compare them side-by-side with filter-based instruments. This has been done by modifying a commercial

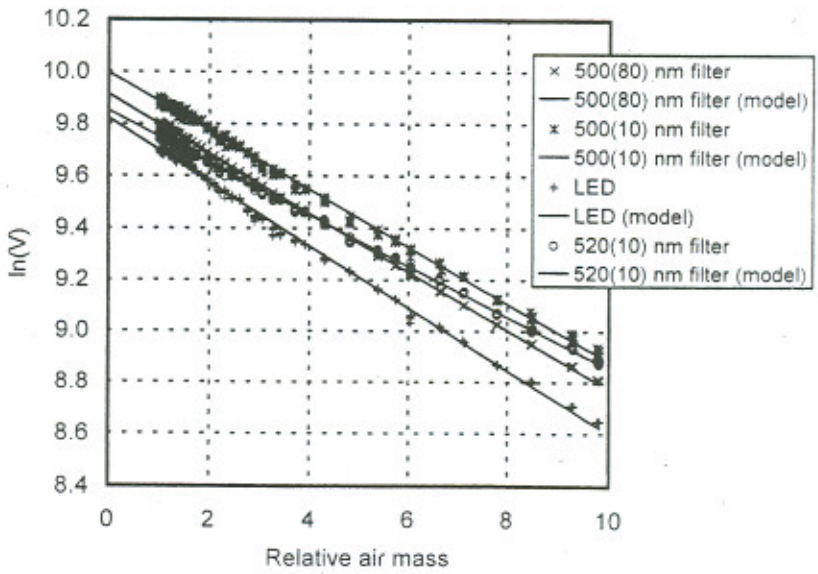

Figure 5. Langley plot data from modified Microtops Sun photometer, at Mauna Loa Observatory (MLO). (See Figure 4.)

MicroTops Sun photometer to make simultaneous measurements with 10-nm filters at 500 nm, 520 nm, and 540 nm, an 80-nm filter centered at 500 nm, and a green LED identical to those used in GLOBE Sun photometers. The spectral response of each of these detectors was determined by using a monochromator and a standard lamp, along with a high-gain amplifier for the LED. The results are shown in Figure 4.

Langley plot calibrations from this instrument have been made at Seguin, Texas, in December 1998 (Mims's site) and at Mauna Loa Observatory (MLO) in May and August, 1999. The Langley data for an especially clear day at MLO (August 27, 1999) are shown in Figure 5. The slope of each Langley plot gives the total optical thickness for that detector. Although it is hard to distinguish among the various detectors, because the channel gains have been adjusted to be all roughly the same, the point of the figure is, in fact, that the Langley data for the LED channel are indistinguishable from data from the filter-based channels.

Figure 6 shows the total optical thickness at MLO on August 27, 1999, as a function of wavelength based on the slopes of the Langley plots and, at 500 nm, the average total optical thickness reported by the AERONET CIMEL Sun photometer at MLO over the time required to collect the Langley data. The solid line is the calculated Rayleigh scattering coefficient corrected for atmospheric pressure at the calibration site. (The pressure correction is relatively large for MLO, with a typical station pressure of about 680 mbar.) For the 10-nm-wide filters, the wavelength is assumed to be the observed peak response wavelength of the filter. (The MicroTop's 500-nm narrowband filter actually peaks at about 503 nm, as shown in Figure 4.) The effective Rayleigh wavelength for the green LED is obtained as described above. For the 80-nm FWHM filter at 500 nm, a similar procedure has been followed based on its observed spectral response as shown in Figure 4; its effective Rayleigh wavelength is about 490 nm.

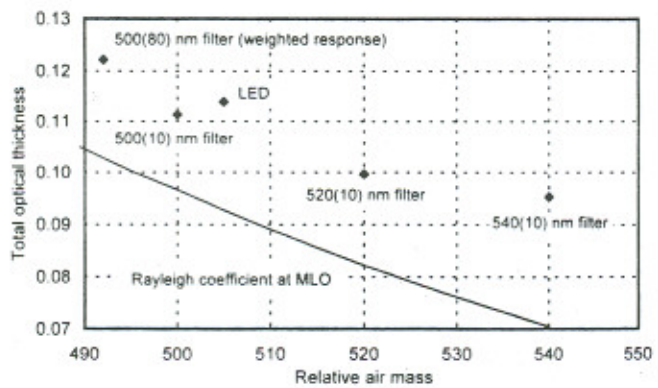

Figure 6. Total optical thickness derived from Langley plots made with modified MicroTops Sun photometer, at Mauna Loa Observatory (See Figures 4 and 5.) The Rayleigh coefficient is corrected to the elevation of MLO.

The significance of Figures 5 and 6 is that they show the extent to which total optical thickness obtained from the LED detector is consistent with data obtained from Sun photometers based on interference filters. The total optical thickness calculated for the LED detector agrees within a few thousandths of an optical thickness unit from what would be expected from a narrowband optical filter with the same center wavelength as the calculated effective Rayleigh wavelength for the LED.

The LED-derived total optical depth is, in fact, closer to the expected value than the value for the 540 nm narrowband filter. The discrepancy in the 540-nm channel can be attributed to the fact that due to a slight misalignment of the collimating tubes in the MicroTops, the data for this filter are noisier by far than for the other filters. Therefore the potential for error in calculating the slope of the regression line is greater. The data in Figure 6 are based on the slope calculated using all the data points shown in Figure 5, even though standard practice is to restrict regression analysis of Langley plot data to relative air masses of from 2 to 6. Applying this restriction to the other channels does not change the results significantly, and for the present purpose, it is not required to realign the collimator for the 540-nm filter and redo these measurements.

6. Transfer Calibrations

It is impractical to perform time-consuming Langley calibrations on large numbers of Sun photometers; GLOBE schools alone could easily require hundreds of these instruments. An alternative strategy is to perform Langley plot calibrations on a few Sun photometers and then to use those as reference instruments to transfer calibrations to other instruments.

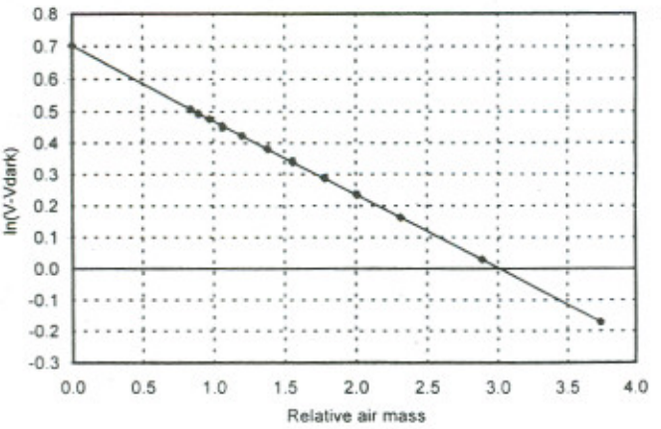

Figure 7. MLO Langley calibration of Global Learning and Observations to Benefit the Environment (GLOBE) sun photometer G2-025, May, 1999. The detector is the Agilent HLMP-D600.

One of the instruments calibrated at MLO in May (G2-025) has been used as a reference for transferring calibrations to other instruments based on side-by-side simultaneous measurements made during the summer of 1999 at Drexel University. Its MLO Langley plot calibration is shown in Figure 7.

In order to assess the reliability of transfer calibrations, several instruments were calibrated at Mauna Loa Observatory (MLO) in May and August of 1999. Of these, two were calibrated in both May and August under significantly different atmospheric conditions. These instruments were then calibrated against G2-025 when they were returned to Drexel University. Two Langley plots for one of these instruments, G1-010, are shown in Figure 8 for May 22 and August 28. The intercepts obtained by extrapolating the regression lines to m=0 are essentially identical. The V_o values shown on Figure 8 are these intercepts corrected to an Earth-Sun distance of 1 AU. (The actual Earth-Sun distances on these two dates are 1.0123 AU on May 22 and 1.0101 AU on August 28.)

The range of aerosol optical thickness (AOT) values calculated from the GLOBE calibration data and from unscreened AERONET values reported online by Holben (aeronet.gsfc.nasa.gov:8080) was about 0.05–0.07 on May 22 and 0.01–0.02 on August 28. The AOT values on August 28 are exceptionally low, near the claimed accuracy for CIMEL aerosol retrievals of about 0.01 AOT unit.

Table 2 gives some statistics for transferring calibrations from instrument G2-025 to six other Sun photometers. The sample standard deviation of these transfers is often less than 0.5% of the average calibration value. The table also includes direct MLO calibrations for some of the instruments. It is not necessarily true that the calibration constant should be taken as the average of all transfer calibrations, but Table 2 demonstrates that the error in doing so is of the order of 1%. For Sun photometers having a good direct Langley calibration, that value has been accepted as the definitive calibration for that instrument.

Because the success of the Haze/Aerosols Project depends on demonstrating not just that LED-based Sun photometers can be calibrated against scientifically accepted standards, but also that students can provide reliable data using these instruments, a partnership was established with Roosevelt High School (RHS), a GLOBE school near NASA's Goddard Space Flight center (GSFC) in Greenbelt, Maryland. The AERONET Sun photometer calibration and maintenance site at GSFC is located only about 1 km from RHS. Over a space of several months, students recorded measurements made with several GLOBE Sun photometers. For each measurement, total atmospheric depth from AERONET's reference CIMEL Sun photometer at GSFC was used to determine the GLOBE Sun photometer's extraterrestrial constant by replacing I with V in (1) and solving for V_o. To do these calculations, it is necessary to interpolate between the CIMEL 500-nm and 675-nm channels and to interpolate in time from available CIMEL measurements to the time at which GLOBE measurements were recorded. Some results are shown in Table 3 for GLOBE Sun photometers G1-008 and G1-010, both of which have been calibrated at MLO, as noted above.

The number in parentheses following the value of V_o for each instrument is the number of measurements in that set. Also shown in Table 3 are the May and August, 1999, MLO calibrations. Each "difference" value shown in the table is the MLO value minus the CIMEL transfer value, divided by the MLO value, expressed as a percent.

As shown in Table 3, the student calibrations agree with the MLO calibrations to within a few percent. This level of agreement is remarkable, considering that the CIMEL measurements must be interpolated both in time and wavelength and that the two instruments have different fields of view. The GLOBE Sun photometer field of view is about 2.5°. The CIMEL field of view is about half that value. Studies have shown that the error in derived AOT introduced by a 2.5° field of view, due to scattered light, is less than 2% under any reasonable measurement conditions [*Reagan et al.*, 1986; *Shaw et al.*, 1973].

7. Temperature Sensitivity

It is well known that photosensitive semiconductors and their associated electronics, including operational amplifiers (op amps) operated as high gain current-to-voltage amplifiers, are temperature sensitive. Thus, the output of any Sun photometer is inherently temperature dependent. This is a problem that can be addressed in a number of ways, and does not directly affect a discussion of how to calibrate Sun photometers and interpret their measurements. However, it is still important to understand the

Table 2. Comparison of Mauna Loa Observatory (MLO) and Transfer Calibrations for Selected Instruments, Using G2-025 as the Reference Standard

Serial Number	Average of Transfer Calibrations	Sample Standard Deviation	n	Standard Deviation as Percent of Calibration Constant	MLO Calibration	Percent Difference
G1-003	3.6749	0.0116	4	0.32	3.6148	-1.6
G1-005	2.4148	0.0073	9	0.30	NA	NA
G1-008	2.0260	0.0040	4	0.19	2.0223	-0.2
G1-011	3.3597	0.0196	8	0.58	NA	NA
G2-024	2.5159	0.0107	6	0.43	2.4860	-1.2
G2-026	1.9668	0.0146	7	0.74	1.9782	0.6

NA, not available.

Table 3. Values of V_o for GLOBE Sun Photometers G1-008 and G1-010 Based on CalibrationsTransferred From a CIMEL Sun Photometer at NASA Goddard Space Flight Center (GSFC) and Langley Plot Calibrations Made at Mauna Loa Observatory (MLO)

Instrument	GSFC, Dec. 15, 1998	GSFC, Dec. 18, 1998	GSFC, Jan. 19, 1999	MLO, May 22, 1999
G1-008	NA	1.996 (5)	2.150 (4)	2.036
Difference	NA	-1.96%	5.60%	
G1-010	2.004 (5)	1.972 (5)	1.980 (3)	1.955
Difference	2.51%	0.87%	1.28%	

limitations that temperature sensitivity might impose on the GLOBE Sun photometer.

Tests conducted by heating and cooling the current GLOBE LED-based Sun photometer, outdoors under realistic field conditions and in the laboratory using a standard lamp light source, have shown that the output voltage sensitivity for a Sun photometer using the D600 emerald green LED is less than 0.003 V/°C. For very clear skies with an AOT of 0.05, a temperature sensitivity of 0.003 V/°C is equivalent to an AOT sensitivity of about 0.0017 AOT units per degree C. At higher AOTs the sensitivity is about 0.002 AOT units per degree Celsius. For an AOT of 0.05, the error is about 3%/°C. For an AOT of 0.25, the error is about 1.8%/°C.

Although this error seems large, especially at low values of AOT (30% for a temperature range of 10°C), it represents worst-case rather than typical performance, as a temperature range of 10° is larger than will occur in practice if the GLOBE measurement protocols are followed. Also, it is worth noting that this level of uncertainty applies not just to LED-based Sun photometers. Even AERONET claims a "total uncertainty in AOT from a newly calibrated field instrument under cloud-free conditions" (conditions rarely met in practice in many parts of the world because of both prevailing weather conditions and the expense of frequent instrument calibrations) of the order of ±0.01 AOT units – ±20% at an AOT of 0.05 [*Holben et al.*, 1998].

The GLOBE requirement for relatively inexpensive instruments precludes active temperature compensation. (Even the AERONET Sun photometers are operated at ambient temperature without active temperature compensation.) The basic strategy is to minimize temperature-related problems by maintaining the Sun photometer as near room temperature as possible while measurements are being made. This is a feasible strategy because GLOBE Sun photometers are not intended to be exposed continuously to outdoor temperatures and direct sunlight. Rather, they are brought outside only for the time required to make measurements, a process that takes less than 10 min. The instrument case is about 15x8x5 cm, so the electronics are somewhat protected from rapid changes in ambient air temperature.

The GLOBE measurement protocols stress the importance of trying to maintain the Sun photometer at room temperature, and they suggest strategies for protecting against temperature fluctuations, such as placing the instrument under the observer's coat between measurements in the winter or encasing the instrument in a protective outer case of white rigid plastic foam and aluminum foil tape during the summer. With only a little care, which our experience has shown that students can and will exercise, temperature fluctuations can be kept to a minimum. The repeatability of MLO and other Langley calibrations made by the authors at different times of the year offers additional evidence that temperature sensitivity is a manageable problem for this instrument.

In terms of instrument design, there are additional no- or low-cost possibilities for dealing with temperature sensitivity. The op amp currently used in the GLOBE Sun photometer produces a dark voltage signal that is linearly proportional to temperature, raising the possibility of providing temperature compensation during data analysis. It may also be possible to reduce the overall circuit gain, which reduces the op amp's gain-dependent temperature drift. Finally, it is possible to minimize temperature sensitivity by using state-of-the-art op amps with very low temperature coefficients. These are not prohibitively expensive, but they require very carefully designed printed circuit boards that are practical only now that the basic design and analysis of the GLOBE Sun photometer has been completed.

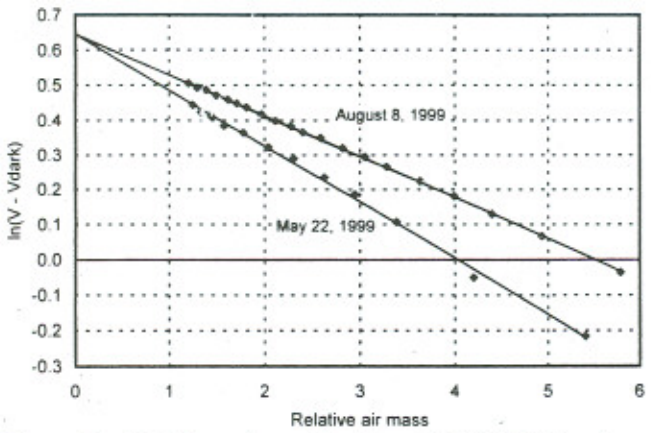

Figure 8. MLO Langley calibrations of GLOBE Sun photometer G1-010 in May and August, 1999. The detector is the Agilent HLMP-D600.

8. Discussion

The results presented here demonstrate that inexpensive LED-based Sun photometers designed for the GLOBE program can be calibrated directly, using the widely accepted Langley plot method, and indirectly against other Sun photometers that use optical filters. In addition, it appears feasible to separate the total optical thickness into components due to aerosols, Rayleigh scattering, and gaseous absorption if the spectral response of their LED detectors is known. The challenge of analyzing measurements obtained with such devices is more than offset by their low cost and long-term stability; these properties make them ideal for use in a global aerosol monitoring network.

A series of calibrations transferred from one GLOBE Sun photometer to another, where the reference instrument has been calibrated at Mauna Loa using the Langley method, shows that it is possible to use a few reference Sun photometers to calibrate large numbers of instruments for distribution to GLOBE schools and other users. An ongoing program to recalibrate Sun photometers at MLO and to redo transfer calibrations is an integral part of the GLOBE Haze/Aerosols Project.

Transfer calibrations based on student data show good agreement with Langley plot calibrations for the same instruments taken at Mauna Loa Observatory even though the CIMEL Sun photometer from which calibrations were transferred has significantly different optical specifications than the GLOBE Sun photometer. Measurements made by students are especially significant because they demonstrate that GLOBE students and other nonspecialists can use these inexpensive instruments to provide reliable aerosol data.

An extensive ground-based network is essential for validating aerosol retrieval algorithms used for processing data from instruments on Earth-monitoring spacecraft such as NASA's recently launched EOS-Terra spacecraft. However the cost of AERONET's CIMEL and other "professional" Sun photometers (including large and ongoing costs for maintenance and calibration) precludes their deployment in a high-density global network. Thus aerosol optical thickness data based on measurements collected by GLOBE students using LED-based Sun photometers can provide a unique and valuable source of information that cannot, as a practical matter, be obtained in any other way.

Notation

$( )_a$	subscript denoting aerosols.
$( )_{a'}$	subscript denoting non-Rayleigh contribution to total atmospheric optical thickness.
A, B, C, D	coefficients in analytic representation of Rayleigh scattering coefficient.
$c(z)$	empirical function relating ozone relative air mass to solar zenith angle.
$( )_{eff}$	subscript denoting effective quantity as weighted by spectral response.
F_o	solar radiation incident at top of the atmosphere, arbitrary units.
$( )_g$	subscript denoting absorption by gases.
I	intensity of light, arbitrary units.
I_o	intensity of light at top of the atmosphere, arbitrary units.
m	relative air mass, dimensionless.
p/p_o	ratio of atmospheric pressure at an observer's elevation and sea level, dimensionless.
r	Earth-Sun distance, astronomical units.
	detector spectral response function, arbitrary units.
R_λ	normalized spectral response for a detector.
$( )_R$	subscript denoting Rayleigh scattering.
$\hat{T}$	wideband transmittance function, dimensionless.
V	voltage, volts.
V_o	Sun photometer voltage at top of the atmosphere (extraterrestrial constant), volts.
z	solar zenith angle, degrees or radians.
α	optical thickness, dimensionless.
λ	wavelength, nanometers or microns.

Acknowledgments. We gratefully acknowledge Brent Holben and Alexander Smirnow, Goddard Space Flight Center, for providing access to total optical depth data from CIMEL Sun photometers at Mauna Loa Observatory and Goddard Space Flight Center; John Barnes, Director, Mauna Loa Observatory, for giving one of us (Mims) access to facilities at MLO; and George Strachan, GLOBE teacher at Roosevelt High School, and his students for providing the measurements used to transfer calibrations from GSFC's CIMEL Sun photometer. This work has been supported by the GLOBE program through National Science Foundation grant 9801806. Any opinions, findings, and conclusions or recommendations expressed in this material are those of the authors and do not necessarily reflect the views of either the GLOBE program or the National Science Foundation.

References

Abbott, C. G., and F. E. Fowle Jr., *Annals of the Astrophysical Observatory of the Smithsonian Institution*, vol. II, part 1, pp.13-64, U.S. Govt. Print. Off., Washington, D. C., 1908.

Bucholtz, A., Rayleigh-scattering calculations for the terrestrial atmosphere, *Appl. Opt., 34*, 2765-2773, 1995.

Dutton, E. G., P. Reddy, S. Ryan, and J. J. DeLuisi, Features and effects of aerosol optical depth observed at Mauna Loa, Hawaii: 1982-1992, *J. Geophys. Res., 99*(D4), 8295-8306, 1994.

Holben, B. N., et al., AERONET — A federated instrument network and data archive for aerosol characterization, *Remote Sens. Environ., 66*, 1-16, 1998.

Iqbal, M., *An Introduction to Solar Radiation*, Academic, San Diego, Calif., 1983.

Meeus, J, *Astronomical Algorithms*. Willmann-Bell, Richmond, Va., 1991.

Mims. F. M., III, Sun photometer with light-emitting diodes as spectrally selective detectors, *Appl. Opt., 31*, 6965-6967, 1992.

Mims, F. M., III, An international haze-monitoring network for students. *Bull. Am. Meteorol. Soc., 80*, 1421-1431, 1999.

Reagan, J. A., L. W. Thomason, B. M. Herman, and J. M. Palmer, Assessment of Atmospheric Limitations on the Determination of the Solar Spectral Constant from Ground-Based Spectroradiometer Measurements. *IEEE Trans. Geosci. Remote Sens., GE-24*(6), 258-265, 1986.

Reagan, J. A., P. A. Pilewskie, I. C. Scott-Fleming, B. J. Herman, and A. Ben-David, Extrapolation of Earth-based solar irradiance measurements to exoatmospheric levels for broad-band and selected absorption-band observations. *IEEE Trans. Geosci. Remote Sens., GE-25*(6), 647-653, 1987.

Shaw, G. E., J. A. Reagan, and B. M. Herman, Investigations of atmospheric extinction using direct solar radiation measurements made with a multiple wavelength radiometer. *J. Appl. Meteorol., 12*, 374-380, 1973.

Thomason, L. W., B. M. Herman, and J. A. Reagan, The effect of atmospheric attenuators with structured vertical distributions on air mass determinations and Langley plot analyses, *J. Atmos. Sci., 40*, 1851-54, 1983.

Volz, F. E., Economical multispectral Sun photometer for measurements of aerosol extinction from 0.44 μm to 1.6 μm and precipitable water, *Appl. Opt., 13*, 1732-1733, 1974.

Young, A. T., Air mass and refraction, *Appl. Opt., 33*, 1108-1110, 1994.

D. R. Brooks, Department of Mathematics and Computer Science, Drexel University, 3141 Chestnut Street, Philadelphia, PA 19104. (dbrooks@mcs.drexel.edu)

F. M. Mims III, Sun Photometer Atmospheric Network, 433 Twin Oak Road, Seguin, TX 78155. (fmims@aol.com)

(Received April 3, 2000; revised August 14, 2000; accepted August 24, 2000.)